HHS Public Access

Author manuscript

Neuroimage. Author manuscript; available in PMC 2018 June 01.

Published in final edited form as:

Neuroimage. 2017 June ; 153: 273–282. doi:10.1016/j.neuroimage.2017.04.008.

Chronic ambulatory electrocorticography from human speech cortex

Vikram R. Rao[a,*,1], **Matthew K. Leonard**[b,c,1], **Jonathan K. Kleen**[a], **Ben A. Lucas**[b,c], **Emily A. Mirro**[d], and **Edward F. Chang**[b,c]

[a]University of California, San Francisco, Department of Neurology, San Francisco, CA 94143

[b]University of California, San Francisco, Department of Neurosurgery, San Francisco, CA 94143

[c]Weill Institute for Neurosciences, University of California, San Francisco, San Francisco, CA 94143

[d]NeuroPace, Inc., Mountain View, CA 94043

Abstract

Direct intracranial recording of human brain activity is an important approach for deciphering neural mechanisms of cognition. Such recordings, usually made in patients with epilepsy undergoing inpatient monitoring for seizure localization, are limited in duration and depend on patients' tolerance for the challenges associated with recovering from brain surgery. Thus, typical intracranial recordings, similar to most non-invasive approaches in humans, provide snapshots of brain activity in acute, highly constrained settings, limiting opportunities to understand long timescale and natural, real-world phenomena. A new device for treating some forms of drug-resistant epilepsy, the NeuroPace RNS® System, includes a cranially-implanted neurostimulator and intracranial electrodes that continuously monitor brain activity and respond to incipient seizures with electrical counterstimulation. The RNS System can record epileptic brain activity over years, but whether it can record meaningful, behavior-related physiological responses has not been demonstrated. Here, in a human subject with electrodes implanted over high-level speech-auditory cortex (Wernicke's area; posterior superior temporal gyrus), we report that cortical evoked responses to spoken sentences are robust, selective to phonetic features, and stable over nearly 1.5 years. In a second subject with RNS System electrodes implanted over frontal cortex (Broca's area, posterior inferior frontal gyrus), we found that word production during a naming task reliably evokes cortical responses preceding speech onset. The spatiotemporal resolution, high signal-to-noise, and wireless nature of this system's intracranial recordings make it a powerful new

[*]Corresponding author. vikram.rao@ucsf.edu.
[1]Authors contributed equally to this work

Conflict of Interest

E.A.M. is an employee of NeuroPace, Inc., manufacturer of the RNS® System, and V.R.R. has received honoraria from NeuroPace for consulting and speaking engagements. The authors declare no targeted funding or compensation from NeuroPace for this study.

approach to investigate the neural correlates of human cognition over long timescales in natural ambulatory settings.

Keywords

human; chronic electrocorticography; ECoG; Wernicke's area; Broca's area; RNS System

Introduction

Human cognitive abilities emerge from patterns of brain activity integrated over multiple timescales (Papo, 2013). Intracranial electroencephalography (iEEG), the direct recording of brain activity with implanted electrodes, is a powerful tool to study cognition, including language, memory, and emotion (Guillory and Bujarski, 2014; Hill et al., 2012; Lachaux et al., 2012). For example, iEEG in human auditory cortex has permitted evaluation of language processing with unprecedented spatiotemporal resolution (Leonard and Chang, 2014; Nourski and Howard, 2015), yielding fundamental insights into mechanisms of speech processing (Bouchard et al., 2013; Leonard et al., 2015; Mesgarani and Chang, 2012).

iEEG recordings can be acquired intraoperatively during tumor resections and chronically in some patients with Parkinson's disease. The opportunity to record iEEG also occurs frequently arises when patients with drug-resistant epilepsy are implanted with intracranial electrodes to localize seizures prior to surgical treatment (Shah and Mittal, 2014). In this context, there are several limitations to iEEG: (1) Experimental sessions are limited by the occurrence of seizures, effects of medication changes, and suboptimal patient participation due to pain, fatigue, and other factors related to the inpatient environment (Hill et al., 2012); (2) Recordings to localize the seizure onset zone rarely extend beyond 1–2 weeks due to infection risk, degradation of signal quality, inability to perform recordings outside the hospital setting, and achievement of clinical goals (Shah and Mittal, 2014); (3) Serial iEEG investigations over time are uncommon, electrode coverage cannot be precisely reproduced during subsequent implantations, and ongoing seizures can distort functional organization in sensory cortex (Serafini et al., 2013).

Thus, despite its utility for examining fine-scale neurophysiological dynamics in humans, traditional iEEG is limited by the challenging circumstances of data collection, and critical questions regarding the long-term dynamics of human cortical activity have remained largely out of reach. For example, auditory cortex contains neural populations that are selective to spectrotemporal acoustic features (Pasley et al., 2012), but it is unknown whether or how these encoding mechanisms change over long timescales. Ideally, direct cortical recordings could be made serially over long periods of time with stably implanted electrodes in a natural context.

Recently, the RNS® System (NeuroPace, Inc.) was approved as a new treatment for seizures arising from brain regions that are not amenable to surgical resection (Bergey et al., 2015; Morrell and Halpern, 2016). The RNS System includes a cranially-implanted programmable neurostimulator connected to two leads that are placed at the seizure focus/foci. Each lead contains four electrode contacts that are used to record and store changes in voltage of

neural populations at a millisecond time scale (electrocorticography; ECoG). The RNS System is fully internalized, and ECoG can be streamed wirelessly in real-time to a laptop computer using a telemetry wand. The neurostimulator detects abnormal patterns of activity and responds by delivering brief, imperceptible pulses of electrical current to inhibit seizure activity. Although the RNS System is a clinical tool, the availability of chronic ECoG in ambulatory patients offers an unprecedented opportunity to study longitudinal patterns of brain activity (Anderson et al., 2015; DiLorenzo et al., 2014; King-Stephens et al., 2015; Smart et al., 2013; Spencer et al., 2016). However, the ability of the RNS System to record physiological responses from eloquent cortical regions has not been reported.

Here, in a subject with RNS System electrodes implanted over the left superior temporal gyrus (STG), we show that passive listening to spoken sentences evokes robust cortical potentials that are selective to specific speech sounds. These responses were stable across recording sessions separated by nearly 1.5 years. To our knowledge, these findings represent the longest timespan over which stimulus-evoked electrophysiological responses have been recorded directly from cortex in an ambulatory human subject. In a second subject with RNS System electrodes implanted over Broca's area in the left inferior frontal gyrus (IFG), we show that word production during a naming task reliably evokes cortical activity that precedes the acoustic onset of speech. The generalizability of this approach across different cortical regions paves the way for studying human cortical physiology over long timescales and in natural, real-world settings.

Materials and Methods

Subjects

This study was carried out in accordance with a protocol approved by the University of California, San Francisco (UCSF) Committee on Human Research. The subjects gave written informed consent in accordance with the Declaration of Helsinki. We obtained iEEG data from two subjects with drug-resistant neocortical epilepsy who were previously implanted with the RNS System in accordance with approved device labeling.

Subject 1 was a 40-year old right-handed female with a ten-year history of drug-resistant focal epilepsy. Her seizures, characterized by bimanual automatisms and aphasia, occurred multiple times a day and did not respond to trials of six anticonvulsant medications. Brain magnetic resonance imaging (MRI) was normal, but scalp EEG localized seizures to the left temporal lobe. She underwent iEEG with left frontotemporal grid electrode coverage, and ictal recordings localized seizures to the posterior left STG. Both extraoperative (during inpatient seizure monitoring) and intraoperative (during grid explantation) electrical stimulation mapping revealed that the seizure onset zone encompassed eloquent language cortex, including parts of classical Wernicke's area (Leonard et al., 2016b). This region was deemed unresectable, so the RNS System was implanted as an alternative treatment option. After RNS System implantation, she became clinically and electrographically seizure-free without need for neurostimulation. She did not experience overt change in her language abilities. In formal neuropsychological testing, her overall level of cognitive functioning was Average, as measured by the Wechsler Abbreviated Scale of Intelligence (WASI; Full-Scale Intelligence Quotient (FSIQ) = 101, 53rd percentile). Her verbal comprehension skills were

Average (Verbal IQ = 94, 34th percentile). On tests of basic verbal intellectual functions, she exhibited Low Average skills for her age in word knowledge (WASI Vocabulary, 16th percentile) and was Average in abstract verbal reasoning (WASI Similarities, 63rd percentile). Her visual confrontation naming skills were impaired for her age and education (Boston Naming Test (BNT) = 49/60, 2nd percentile), while her auditory naming skills fell in the Average range (Auditory Naming Test (ANT) = 49/50, 27th percentile).

Subject 2 was an 18-year old left-handed female with drug-resistant focal epilepsy since age 5. Her seizures involved behavioral arrest, expressive language difficulty, choking, and right upper extremity clonic movements, occasionally progressing to convulsions. Seizures occurred daily and were not controlled by trials of nine anticonvulsant medications. Brain MRI was normal, but scalp EEG monitoring indicated seizures arising from the left hemisphere. iEEG with left hemispheric grid electrodes revealed seizures arising from the IFG, a region co-localizing with speech production cortex (classical Broca's area) as determined by electrical stimulation mapping. The subject was left-handed, but blood oxygen level-dependent functional MRI (BOLD-fMRI) language mapping revealed left hemispheric lateralization of expressive and receptive language function. She underwent formal neuropsychological testing at age 13. On the Wechsler Intelligence Scale for Children, Fourth Edition (WISC-IV), measures of verbal intellectual ability were within the Low Average to Average range (Verbal Comprehension Index Score (prorated) = 27, 37th percentile), and measures of non-verbal ability were within the Borderline range (Perceptual Reasoning Index Score (prorated) = 17, 4th percentile). On language testing, semantic verbal fluency, verbal categorization, single-word receptive vocabulary, rapid color naming, and speeded color-word reading all were within the Low Average to Average range. Phonemic fluency (Delis-Kaplan Executive Function System (D-KEFS) Letter Fluency = 15, 5th percentile) and confrontation naming (Peabody Picture Vocabulary Test, Fourth Edition (PPVT-4) = 22, 7th percentile) were Borderline. This subject was previously implanted with a vagus nerve stimulator (VNS; Cyberonics, Inc., Houston, TX) for treatment of seizures. VNS settings were not changed during the study period. RNS System recording experiments were carried out 12 days after neurostimulator implantation, before the responsive stimulation function of the device was enabled.

RNS System

Subjects were implanted with the RNS System (NeuroPace, Inc., Mountain View, CA) and electrodes were placed at the seizure onset zone as determined by prior iEEG. RNS System detection settings involved a line length detector applied to ECoG channels 1 and 3 (short-term window 4.096 sec, long-term window 2 min, threshold ratio for short-/long-term window average line length was 50% for Subject 1 and 75% for Subject 2). For Subject 1, detection settings were held constant between the 2 and 18.5 months post-implant (MPI) timepoints. Responsive stimulation was not enabled on the device during the study period for Subject 1 because she remained free of clinical and electrographic seizures after implantation. Subject 2 was recorded at a single timepoint just before responsive stimulation was enabled on the device, and she continues to have seizures. Wireless wand telemetry to stream real-time ECoG during stimulus presentation was performed in accordance with normal clinical use of the device. The maximum length of each streamed ECoG file is 4 min.

For their convenience, Subjects were recorded during regular outpatient clinic appointments, and so testing time was limited to approximately 20 min per session.

Electrode Localization

Cortical surface anatomy was estimated from T1-weighted MRI using FreeSurfer (Dale et al., 1999). To determine the locations of the RNS System electrodes, a post-implantation head computed tomography (CT) scan was co-registered with the MRI, and the coordinates of each electrode centroid were computed in cortical surface space using custom Matlab (Mathworks, Inc., Natick, MA) and Python (Python Software Foundation, Beaverton, OR) code.

Tasks/Stimuli

Subject 1 passively listened to 499 complete sentences from the TIMIT speech corpus (Garofalo et al., 1993) while real-time ECoG was recorded using the wireless telemetry system. These sentences contain the full inventory of English speech sounds and have been used previously to characterize the phonetic sensitivity of neural populations across the posterior STG (Mesgarani et al., 2014). Each complete TIMIT sentence was considered a single trial, except for phonetic analyses. The same TIMIT stimuli were presented during conventional iEEG and RNS System recordings.

In a similar outpatient recording setup, Subject 2 was instructed to listen to sentences describing a particular word and then to state the word that best fit the description. Example sentences include: “An animal that says meow,” or “An insect that makes honey” (to which the subject would say “cat” and “bee”, respectively). This task is similar to a previously reported Auditory Naming Task (Hamberger and Seidel, 2003), although we modified it so that sentences had a consistent noun-verb-noun structure. Each description-word (stimulus-speech response) pair was considered a single trial, and the subject performed 50 total trials. If the subject could not think of the word, we allowed up to approximately 10 seconds of response time before moving to the next trial.

ECoG Analysis & Statistics

Raw ECoG files were obtained from NeuroPace, Inc. in accordance with data transfer protocols approved by UCSF. Four-channel bipolar-referenced ECoG was recorded by the neurostimulator with 250 Hz sampling rate and analog high-pass filter at 4 Hz. Data were low-pass filtered at 125 Hz. For EMU recordings, data were sampled at 3051 Hz and low-pass filtered at 1500 Hz.

Since there are no auxiliary inputs on the RNS System that can be used for audio or stimulus markers, we used two methods for time-locking neural responses to speech. For Subject 1, we divided the sentences into 10 WAV files that each contained approximately 50 stimuli. To identify the lag between the start of the ECoG recording and the onset of each audio file, we used the fact that posterior STG neural populations tend to show pronounced responses to auditory onsets. Since the delay between individual sentence onsets was known from the audio, we calculated the average event-related potentials (ERPs) in the high-gamma signal (see below), and identified the peak latency of this response. This allowed us to determine

the offset between the start of the ECoG recording and the presentation of the first (and hence, all subsequent) sentences within each block. Supplementary Fig. 1 uses data with known offsets to validate this method. To compensate for known conduction delays in the human auditory system, based on our previous work (Chang et al., 2011), we added 120 ms to this lag to arrive at realistic temporal profiles of auditory evoked responses.

To time-lock ECoG during the Auditory Naming Task, a video of the clock and user interface from the laptop streaming ECoG data was captured during the recording, including user interface events and ambient audio from the task. Audio events, including pre-recorded sentence stimuli and speech responses, were detected in the audio track via circular convolution and audio envelope thresholding, respectively. Inspection of the video frames (29.97 frames per second) provided a mechanism to link the ECoG recording onset with the audio. The overall offset from this linking method was likely less than 60 msec (within 1 or 2 video frames), far shorter than the duration of the high-gamma responses described. Scaling of sampling rates for audio and ECoG data made this offset error relatively consistent for stimuli and speech events across the recording, minimizing any further offset error during trial averaging.

Auditory evoked responses (timelocked to stimulus onset) were computed for the raw voltage signals and normalized for each electrode at each recording time. To compute spectral decompositions of the neural data for both subjects, we calculated the Hilbert transform of 35 bands with center frequencies increasing on a log scale from 4–120 Hz. This data was pre-filtered (Gaussian filter) with corresponding band window sizes increasing logarithmically from 0.45 to 6.12 Hz, respectively. To provide estimates of normalized power, the analytic amplitude of each frequency band was then z-scored relative to the mean and standard deviation of the pre-stimulus baseline period for each trial from [−500 0]ms. After frequency decomposition, data were downsampled to 100 Hz. To examine effects in the high-gamma frequency range, the data from the frequency bands (six total, logarithmically spaced as noted above) between 70 and 120 Hz were averaged. Power spectral density functions for each electrode were computed using the ‘pwelch’ function in Matlab and calculated from 4–120 Hz, just below the Nyquist frequency of the recordings.

To examine phonetic feature encoding, the TIMIT stimuli were parsed according to phonemes and categorized by four phonetic features previously shown to be encoded in posterior STG: fricatives (e.g., /s/, /z/, /sh/), plosives (e.g., /b/, /d/, /k/), nasals (e.g., /m/, /n/), and vowels (e.g., /aa/, /iy/, /uw/) (Mesgarani et al., 2014). Responses to each phoneme in each feature category across all instances in the data set were averaged to determine whether electrodes were selective to specific features.

Results

The first subject was implanted with the RNS System with four subdural cortical strip leads, three overlying the superior and middle temporal gyri and a fourth lead placed subtemporally (Fig. 1A). The superior two strips, overlying the left STG (encompassing Wernicke’s area), were connected to the neurostimulator (Fig. 1B) and ECoG was recorded by the device. Remarkably, the subject subsequently became seizure-free (now over two

years), as can rarely occur after intracranial monitoring (Katariwala et al., 2001; Roth et al., 2012). While the neurostimulator continued to record and store ECoG, the responsive stimulation function of the device was never enabled.

The absence of seizures or electrical stimulation in this subject afforded a unique opportunity to record physiological responses directly from eloquent cortex over long periods of time. We first verified the quality of ECoG recordings from the RNS System. The ECoG background activity of cerebral cortex resembles broadband noise (Freeman and Zhai, 2009), and power spectral density (PSD) plots of RNS System ECoG signals showed the expected power-law form (Miller et al., 2009) (Fig. 1C). These measurements were highly stable between the two recording sessions, which occurred at 2 and 18.5 months post-implant (MPI). Lead impedances increased over 16 weeks post-implant and were then stable in long-term follow-up (Fig. 2), consistent with previous studies on the RNS System electrode-tissue interface (Sillay et al., 2013; Wu et al., 2013). The stability of PSD plots between timepoints (Fig. 1C) argues against significant frequency-dependent effects of changes in electrode impedances.

The electrodes were directly over the left STG, an auditory region that is critical for high-level speech comprehension. Therefore, we investigated whether acoustic speech input evokes complex auditory responses that could be recorded by the device. During a routine outpatient clinic appointment at 2 MPI, we used wireless wand telemetry to stream real-time ECoG while the subject passively listened to 499 spoken sentences. Event-related potentials to sentence onsets were apparent in the raw voltage traces (broadband ECoG signal) for all four channels (Fig. 3A, green traces). To determine the long-term stability of these responses, we performed an identical recording session at 18.5 MPI and found similar responses on each electrode (Fig. 3A, blue traces; blue and green shading indicate timepoints where $p < 0.05$, Bonferroni corrected for timepoints using a one-way t-test, two-tailed). The correlations between the two recording sessions for each electrode are shown in Table 1 and demonstrate robust stability of broadband ECoG responses across time.

To examine the spectral characteristics of this auditory-evoked neural activity, we decomposed the broadband signal into 35 frequencies from 4–120 Hz (just below the Nyquist frequency of the recordings). At both 2 and 18.5 MPI timepoints, average sentence-evoked neural spectrograms revealed an increase in high gamma activity (60–120 Hz), which was maximal in electrodes located over the posterior dorsal STG (e2; Fig 3B, purple arrows), among other changes in lower frequencies (one-way z-test $p<0.05$, two-tailed, Bonferroni corrected for timepoints and frequency bins). This area has been directly implicated in representing phonetic features of speech (Leonard and Chang, 2014) and high gamma activity, which is thought to reflect neuronal spiking and cortical activation (Ray et al., 2008), is known to correlate strongly with acoustic and phonetic representations in posterior STG. Of note, dynamic changes in lower frequencies were readily observable in the spectrograms for this task as well. There was an initial increase and subsequent decrease in beta (12–30 Hz) power in electrodes e1, e2, and e4 (Fig. 3B). A large increase in theta (4–8 Hz) power was also observed, particularly at the 18.5 MPI timepoint (Fig. 3B). As the subtraction of neural spectrograms illustrates, only a small early effect at ~20Hz differed significantly across sessions (two-way t-test $p<0.05$, two-tailed, Bonferroni corrected for

timepoints and frequency bins; uncorrected p<0.00017). The correlations between the two recording sessions for each electrode are shown in Table 2 and demonstrate robust stability of ECoG responses across frequency bands.

As with traditional iEEG recordings of high-gamma activity, the robust signal-to-noise ratio in the RNS System ECoG data afforded single-trial resolution. We observed that each of the approximately 450 artifact-free sentences evoked a sharp onset response, and activity remained elevated above baseline until sentence offset (Fig. 4A). Averaging over all sentence trials, we found that high gamma activity peaks 150 ms after sentence onset (Fig. 4B). To examine the temporal properties of these responses, we correlated the high-gamma activity on each trial with the amplitude envelope of the sentence audio. We observed a peak in the cross-correlation at short lags (Fig. 4C), a feature of the auditory cortex response specifically to speech sounds (Kubanek et al., 2013). The correlation between the timecourses at 2 MPI and 18.5 MPI was robust (r=0.95, p=3.58e-190, 95% CI = [0.94 0.96]). The cortical response was more robust at 18.5 MPI than at 2 MPI (Fig. 4B, C), but the fact that the timecourse of the response was qualitatively similar at these timepoints suggests highly stable language representation, consistent with the lack of changes in the subject's language behavior.

We next sought to validate the observed auditory responses by comparison with speech recordings made during the subject's iEEG evaluation in the epilepsy monitoring unit (EMU) (Fig. 5A). The pattern of auditory event-related potentials recorded with the RNS System was qualitatively similar to conventional iEEG (Fig. 5B), with small differences likely owing to the fact that iEEG and RNS System electrodes were not precisely anatomically co-localized. Single-trial data from EMU recordings (Supplementary Fig. 2) revealed robust high-gamma responses with normalized response values comparable to RNS System recordings (Fig. 4A).

These average evoked responses demonstrate that the RNS System can record activity evoked by acoustic input. However, it is unknown whether these recordings have the spatial and temporal resolution to examine the tuning of underlying neural populations to specific speech sound features, and whether this tuning is stable across long timescales. In particular, STG neural populations are tuned to acoustic features of speech sounds, such as fricatives (e.g., /s/, /z/, /sh/), plosives (e.g., /b/, /d/, /k/), nasals (e.g., /m/, /n/), and vowels (e.g., /aa/, /iy/, /uw/) (Mesgarani et al., 2014). To date, these fine-scale speech representations have not been examined longitudinally, which is critical for understanding how primary and secondary sensory areas are affected by experience-dependent functional reorganization over time (Buonomano and Merzenich, 1998). In the broadband ECoG signal recorded from dorsal STG, we observed selectivity to these four key phonetic feature classes (Fig. 6A). Remarkably, this pattern of phonetic feature selectivity was consistent across nearly 1.5 years of recordings (Fig. 6B; r=0.45, p=1.48e-18, 95% CI = [0.31 0.54]).

Having established that the RNS System can stably record meaningful physiological responses from speech-auditory cortex over long timescales, we next explored the generalizability of this approach by investigating another eloquent cortical region involved in speech. In the second subject, iEEG monitoring during presurgical evaluation for drug-

resistant epilepsy revealed a seizure focus in left inferior frontal gyrus (IFG). This area co-localized with Broca's area, which could not be safely resected, and so the RNS System was implanted for clinical purposes with two four-contact cortical strip leads over the seizure onset zone (Fig. 7A).

Cortical activation in Broca's area occurs during naming paradigms and other tasks requiring word production (Cannestra et al., 2000; Flinker et al., 2015; Sahin et al., 2009). To determine whether evoked cortical responses could be recorded from this area, we used the RNS System to stream real-time wireless ECoG while the subject engaged in an auditory naming task (see Materials & Methods). The subject's accuracy across 50 trials was 94%, and mean reaction time was 2.4794 seconds (SEM ±0.358 sec; median 1.538). One of the recorded channels (Fig. 7A) showed a marked increase in high gamma power in the seconds prior to speech onset and a decrease in activity during active speech (Fig. 7B), consistent with the known response profile of Broca's area (Flinker et al., 2015). Single-trial analysis (Fig. 7C) confirmed that, despite variable latency from word cue to speech production, task-evoked high gamma activity is constrained to the pre-articulation period, a feature that distinguishes this region from adjacent speech motor cortex (Flinker et al., 2015).

Discussion

Chronic intracranial recordings with RNS System electrodes over speech-auditory cortex revealed responses to speech that were robust, selective to phonetic features, and stable over nearly 1.5 years. To our knowledge, this is the longest timespan over which an implanted electrode system has been used to record stimulus-evoked physiological responses directly from cortex in an ambulatory human subject. Although the long-term stability of cortical speech representations in adults is predicted by known auditory critical periods (Kral, 2013), our findings provide the first direct evidence of this stability with chronic ambulatory electrocorticography. In particular, we demonstrate that not only are the same general cortical regions active, but they show the same fine-scale tuning for acoustic-phonetic features of speech. Given the relatively rare circumstances in which a chronic recording device is implanted without also enabling stimulation features that may induce instability in the underlying neural circuits, this data set also provides a unique view of the fine spatiotemporal properties of sensory/perceptual auditory processes over long timescales. In a different subject, RNS System recordings from another hub of the human cortical speech network, Broca's area, also revealed evoked cortical responses with high temporal specificity. This highlights the utility of the RNS System as a research tool for diverse studies of human cortical physiology.

We observed dynamics in lower frequency bands, including task-related fluctuations in theta and beta bands in Subject 1 that were statistically significant (Fig. 3). These fluctuations parallel those seen in Wernicke's area in a study measuring speech-related responses to single words (Canolty et al., 2007), and different frequencies may reflect distinct levels of speech processing (Mai et al., 2016), though we cannot rule out effects related to changes in electrode impedances (Fig. 2). In this study, we focused on the HG band given its strong association with cortical activation (Ray et al., 2008) and relevance for linguistic neurophysiology (Leonard et al., 2016a; Leonard et al., 2016b; Steinschneider et al., 2011),

though analysis of lower frequency dynamics would also be possible with data acquired by the RNS System. Future experiments employing a more diverse array of tasks could determine the specificity of the observed responses for language, motor preparation, or other aspects of cognitive processing (Udden and Bahlmann, 2012).

Proper observation of a given process requires that the observation time is much longer than any scale within the system (Papo, 2013). For some neural processes, like cortical reorganization after injury, the requisite observation timescale may be months to years (Chelette et al., 2013; Dilks et al., 2007; Kerr et al., 2011). Despite recent technological advances in long-term recording equipment for animal studies (Okun et al., 2016), obtaining stable intracranial recordings over such durations remains challenging in animals (Blake et al., 2006; Kato et al., 2015) and was, until recently, impossible in humans (Brumberg et al., 2010; Kennedy et al., 2011). As a result, studies of long-term neuroplasticity in humans have employed non-invasive imaging (Sala-Llonch et al., 2015; Zatorre et al., 2012) or brain stimulation (Freitas et al., 2011), *ex vivo* physiology (Andersson et al., 2016), and cross-sectional study design (Freitas et al., 2011; Skoe et al., 2015).

First approved for clinical use in 2013, the RNS System has become an important tool for treating some patients with drug-resistant epilepsy whose seizures are not amenable to surgical resection (Morrell and Halpern, 2016). Recently, several reports have highlighted the diagnostic power of the RNS System, using chronic ECoG recorded by the device to characterize longitudinal dynamics of epileptiform activity (DiLorenzo et al., 2014; King-Stephens et al., 2015; Mackow et al., 2016; Smart et al., 2013). Here, we extend the research applications of the RNS System by recording fine-grained physiological responses from eloquent cortex over long periods of time. This opens the door for future investigations of plasticity and other fundamental cortical mechanisms that operate on long timescales. Although an upper limit for chronic recordings with the RNS System has not been defined, broad markers of epileptiform activity in ECoG recordings are resilient in studies of patients implanted for up to 7.1 years (King-Stephens et al., 2015). The ability to perform intracranial recordings in ambulatory patients who have fully recovered from surgery also provides many experimental advantages that are not possible with other methods.

The ‘implant effect’ refers to a window of time after device implantation, usually not exceeding six months, during which lead impedances are stabilizing (Fig. 2) and cortical responses may be suppressed for reasons that remain unclear (Lane et al., 2016). This could potentially explain why evoked high gamma activity was more robust at 18.5 MPI than at 2 MPI (Fig. 4B, C). Other possibilities include resolution of local edema, subtle electrode shift or settling over time, and remission of epilepsy. The latency from sentence onset of some auditory responses also differed slightly between the two timepoints (Fig. 6A, B). Although this could be due to a physiological change, we suspect that this actually reflects some imprecision in aligning ECoG recordings with stimulus onset.

The lack of a straightforward means of time-locking ECoG to task events is a major limitation of this study. We attempted multiple methods to circumvent this issue, including reliance on the neurophysiological responses themselves (HG peak latencies (Chang et al., 2011)) and temporal association via audio/visual recordings of task events and the RNS

System laptop display. Both of these methods likely reduce the strength of responses due to temporal blurring. This becomes more relevant as the frequency of interest increases but it also has implications for phase analyses of lower frequencies. The methods we utilized are not intended to be long-term solutions to this issue. More reliable methods are in active development (Tcheng et al., 2015) and should facilitate use of the RNS System for translational research applications.

Our study has other limitations, including the sparse electrode coverage in the current generation of the RNS System. The spatial resolution afforded by the device might be insufficient for comparing in detail the functions of multiple brain regions. As such, the RNS System may be best suited for research applications that leverage the chronicity of intracranial recordings and depend less on extensive spatial sampling. Relatively low data sampling rate is another limitation of the RNS System as a research tool, as sampling rate can affect determination of peak frequencies even below the Nyquist limit (Gliske et al., 2016). For clinical purposes, RNS System electrodes are placed only at the seizure focus or foci, where normal physiological responses could be distorted, while conventional iEEG typically includes sampling of some cortical areas that are not involved in seizure generation. Despite these caveats, it is striking that we observed speech-evoked neurophysiological responses that are highly similar to responses recorded with more established recording methods (Fig. 5).

We report on two subjects with electrodes sampling cortical language areas, but other brain regions, including deeper structures like the hippocampus, will need to be tested in the future. Neither subject had yet received stimulation by the RNS System at the time of these recordings, so the potential effects of chronic neurostimulation on sensory representations cannot be answered from our data. This remains an area of active exploration in subjects who have stimulation enabled. Evidence of stimulation-induced functional reorganization could shed light on the therapeutic mechanisms of chronic neurostimulation.

Supplementary Material

Refer to Web version on PubMed Central for supplementary material.

Acknowledgments

This work was supported by National Institutes of Health (NIH) grants R01-DC012379 (E.F.C.), R25NS070680-07 (J.K.K.), and F32-DC013486 (M.K.L.) and by a Kavli Institute for Brain and Mind Innovative Research grant (M.K.L.). Research reported in this publication was supported by the National Institute of Neurological Disorders and Stroke of the NIH under Award Number U01NS098971. The content is solely the responsibility of the authors and does not necessarily represent the official views of the NIH. E.F.C. is a New York Stem Cell Foundation – Robertson Investigator. This research was supported by The New York Stem Cell Foundation. We thank Liberty Hamilton for providing pre-processing code.

References

Anderson CT, Tcheng TK, Sun FT, Morrell MJ. Day-Night Patterns of Epileptiform Activity in 65 Patients With Long-Term Ambulatory Electrocorticography. J Clin Neurophysiol. 2015; 32:406–412. [PubMed: 26426769]

Andersson M, Avaliani N, Svensson A, Wickham J, Pinborg LH, Jespersen B, Christiansen SH, Bengzon J, Woldbye DP, Kokaia M. Optogenetic control of human neurons in organotypic brain cultures. Sci Rep. 2016; 6:24818. [PubMed: 27098488]

Bergey GK, Morrell MJ, Mizrahi EM, Goldman A, King-Stephens D, Nair D, Srinivasan S, Jobst B, Gross RE, Shields DC, Barkley G, Salanova V, Olejniczak P, Cole A, Cash SS, Noe K, Wharen R, Worrell G, Murro AM, Edwards J, Duchowny M, Spencer D, Smith M, Geller E, Gwinn R, Skidmore C, Eisenschenk S, Berg M, Heck C, Van Ness P, Fountain N, Rutecki P, Massey A, O'Donovan C, Labar D, Duckrow RB, Hirsch LJ, Courtney T, Sun FT, Seale CG. Long-term treatment with responsive brain stimulation in adults with refractory partial seizures. Neurology. 2015; 84:810–817. [PubMed: 25616485]

Blake DT, Heiser MA, Caywood M, Merzenich MM. Experience-dependent adult cortical plasticity requires cognitive association between sensation and reward. Neuron. 2006; 52:371–381. [PubMed: 17046698]

Bouchard KE, Mesgarani N, Johnson K, Chang EF. Functional organization of human sensorimotor cortex for speech articulation. Nature. 2013; 495:327–332. [PubMed: 23426266]

Brumberg JS, Nieto-Castanon A, Kennedy PR, Guenther FH. Brain-Computer Interfaces for Speech Communication. Speech Commun. 2010; 52:367–379. [PubMed: 20204164]

Buonomano DV, Merzenich MM. Cortical plasticity: from synapses to maps. Annu Rev Neurosci. 1998; 21:149–186. [PubMed: 9530495]

Cannestra AF, Bookheimer SY, Pouratian N, O'Farrell A, Sicotte N, Martin NA, Becker D, Rubino G, Toga AW. Temporal and topographical characterization of language cortices using intraoperative optical intrinsic signals. Neuroimage. 2000; 12:41–54. [PubMed: 10875901]

Canolty RT, Soltani M, Dalal SS, Edwards E, Dronkers NF, Nagarajan SS, Kirsch HE, Barbaro NM, Knight RT. Spatiotemporal dynamics of word processing in the human brain. Front Neurosci. 2007; 1:185–196. [PubMed: 18982128]

Chang EF, Edwards E, Nagarajan SS, Fogelson N, Dalal SS, Canolty RT, Kirsch HE, Barbaro NM, Knight RT. Cortical spatio-temporal dynamics underlying phonological target detection in humans. J Cogn Neurosci. 2011; 23:1437–1446. [PubMed: 20465359]

Chelette KC, Carrico C, Nichols L, Sawaki L. Long-term cortical reorganization following stroke in a single subject with severe motor impairment. NeuroRehabilitation. 2013; 33:385–389. [PubMed: 23949080]

Dale AM, Fischl B, Sereno MI. Cortical surface-based analysis. I. Segmentation and surface reconstruction. Neuroimage. 1999; 9:179–194. [PubMed: 9931268]

Dilks DD, Serences JT, Rosenau BJ, Yantis S, McCloskey M. Human adult cortical reorganization and consequent visual distortion. J Neurosci. 2007; 27:9585–9594. [PubMed: 17804619]

DiLorenzo DJ, Mangubat EZ, Rossi MA, Byrne RW. Chronic unlimited recording electrocorticography-guided resective epilepsy surgery: technology-enabled enhanced fidelity in seizure focus localization with improved surgical efficacy. J Neurosurg. 2014; 120:1402–1414. [PubMed: 24655096]

Flinker A, Korzeniewska A, Shestyuk AY, Franaszczuk PJ, Dronkers NF, Knight RT, Crone NE. Redefining the role of Broca's area in speech. Proc Natl Acad Sci U S A. 2015; 112:2871–2875. [PubMed: 25730850]

Freeman WJ, Zhai J. Simulated power spectral density (PSD) of background electrocorticogram (ECoG). Cogn Neurodyn. 2009; 3:97–103. [PubMed: 19003455]

Freitas C, Perez J, Knobel M, Tormos JM, Oberman L, Eldaief M, Bashir S, Vernet M, Pena-Gomez C, Pascual-Leone A. Changes in cortical plasticity across the lifespan. Front Aging Neurosci. 2011; 3:5. [PubMed: 21519394]

Garofalo, JS., Lamel, LF., Fisher, WM., Fiscus, JG., Pallett, DS., Dahlgren, NL. TIMIT Acoustic-Phonetic Continuous Speech Corpus. Philadelphia: Linguistic Data Consortium; 1993. p. LDC93S1

Gliske SV, Irwin ZT, Chestek C, Stacey WC. Effect of sampling rate and filter settings on High Frequency Oscillation detections. Clin Neurophysiol. 2016; 127:3042–3050. [PubMed: 27472539]

Guillory SA, Bujarski KA. Exploring emotions using invasive methods: review of 60 years of human intracranial electrophysiology. Soc Cogn Affect Neurosci. 2014; 9:1880–1889. [PubMed: 24509492]

Hamberger MJ, Seidel WT. Auditory and visual naming tests: normative and patient data for accuracy, response time, and tip-of-the-tongue. J Int Neuropsychol Soc. 2003; 9:479–489. [PubMed: 12666772]

Hill NJ, Gupta D, Brunner P, Gunduz A, Adamo MA, Ritaccio A, Schalk G. Recording human electrocorticographic (ECoG) signals for neuroscientific research and real-time functional cortical mapping. J Vis Exp. 2012

Katariwala NM, Bakay RA, Pennell PB, Olson LD, Henry TR, Epstein CM. Remission of intractable partial epilepsy following implantation of intracranial electrodes. Neurology. 2001; 57:1505–1507. [PubMed: 11673602]

Kato HK, Gillet SN, Isaacson JS. Flexible Sensory Representations in Auditory Cortex Driven by Behavioral Relevance. Neuron. 2015; 88:1027–1039. [PubMed: 26586181]

Kennedy P, Andreasen D, Bartels J, Ehirim P, Mao H, Velliste M, Wichmann T, Wright J. Making the lifetime connection between brain and machine for restoring and enhancing function. Brain Machine Interfaces: Implications for Science, Clinical Practice and Society. 2011; 194:1–25.

Kerr AL, Cheng SY, Jones TA. Experience-dependent neural plasticity in the adult damaged brain. J Commun Disord. 2011; 44:538–548. [PubMed: 21620413]

King-Stephens D, Mirro E, Weber PB, Laxer KD, Van Ness PC, Salanova V, Spencer DC, Heck CN, Goldman A, Jobst B, Shields DC, Bergey GK, Eisenschenk S, Worrell GA, Rossi MA, Gross RE, Cole AJ, Sperling MR, Nair DR, Gwinn RP, Park YD, Rutecki PA, Fountain NB, Wharen RE, Hirsch LJ, Miller IO, Barkley GL, Edwards JC, Geller EB, Berg MJ, Sadler TL, Sun FT, Morrell MJ. Lateralization of mesial temporal lobe epilepsy with chronic ambulatory electrocorticography. Epilepsia. 2015; 56:959–967. [PubMed: 25988840]

Kral A. Auditory critical periods: a review from system's perspective. Neuroscience. 2013; 247:117–133. [PubMed: 23707979]

Kubanek J, Brunner P, Gunduz A, Poeppel D, Schalk G. The tracking of speech envelope in the human cortex. PLoS One. 2013; 8:e53398. [PubMed: 23408924]

Lachaux JP, Axmacher N, Mormann F, Halgren E, Crone NE. High-frequency neural activity and human cognition: past, present and possible future of intracranial EEG research. Prog Neurobiol. 2012; 98:279–301. [PubMed: 22750156]

Lane MA, Kahlenberg CA, Li Z, Kulandaival K, Secore KL, Thadani VM, Bujarski KA, Kobylarz EJ, Roberts DW, Tosteson TD, Jobst BC. The implantation effect: delay in seizure occurrence with implantation of intracranial electrodes. Acta Neurol Scand. 2016

Leonard MK, Baud MO, Sjerps MJ, Chang EF. Perceptual restoration of masked speech in human cortex. Nat Commun. 2016a; 7:13619. [PubMed: 27996973]

Leonard MK, Bouchard KE, Tang C, Chang EF. Dynamic encoding of speech sequence probability in human temporal cortex. J Neurosci. 2015; 35:7203–7214. [PubMed: 25948269]

Leonard MK, Cai R, Babiak MC, Ren A, Chang EF. The peri-Sylvian cortical network underlying single word repetition revealed by electrocortical stimulation and direct neural recordings. Brain Lang. 2016b

Leonard MK, Chang EF. Dynamic speech representations in the human temporal lobe. Trends Cogn Sci. 2014; 18:472–479. [PubMed: 24906217]

Mackow MJ, Krishnan B, Bingaman WE, Najm IM, Alexopoulos AV, Nair DR. Increased caffeine intake leads to worsening of electrocorticographic epileptiform discharges as recorded with a responsive neurostimulation device. Clin Neurophysiol. 2016; 127:2341–2342. [PubMed: 27178850]

Mai G, Minett JW, Wang WS. Delta, theta, beta, and gamma brain oscillations index levels of auditory sentence processing. Neuroimage. 2016; 133:516–528. [PubMed: 26931813]

Mesgarani N, Chang EF. Selective cortical representation of attended speaker in multi-talker speech perception. Nature. 2012; 485:233–236. [PubMed: 22522927]

Mesgarani N, Cheung C, Johnson K, Chang EF. Phonetic feature encoding in human superior temporal gyrus. Science. 2014; 343:1006–1010. [PubMed: 24482117]

Miller KJ, Sorensen LB, Ojemann JG, den Nijs M. Power-law scaling in the brain surface electric potential. PLoS Comput Biol. 2009; 5:e1000609. [PubMed: 20019800]

Morrell MJ, Halpern C. Responsive Direct Brain Stimulation for Epilepsy. Neurosurg Clin N Am. 2016; 27:111–121. [PubMed: 26615113]

Nourski KV, Howard MA 3rd. Invasive recordings in the human auditory cortex. Handb Clin Neurol. 2015; 129:225–244. [PubMed: 25726272]

Okun M, Lak A, Carandini M, Harris KD. Long Term Recordings with Immobile Silicon Probes in the Mouse Cortex. PLoS One. 2016; 11:e0151180. [PubMed: 26959638]

Papo D. Time scales in cognitive neuroscience. Front Physiol. 2013; 4:86. [PubMed: 23626578]

Pasley BN, David SV, Mesgarani N, Flinker A, Shamma SA, Crone NE, Knight RT, Chang EF. Reconstructing speech from human auditory cortex. PLoS Biol. 2012; 10:e1001251. [PubMed: 22303281]

Ray S, Crone NE, Niebur E, Franaszczuk PJ, Hsiao SS. Neural correlates of high-gamma oscillations (60–200 Hz) in macaque local field potentials and their potential implications in electrocorticography. J Neurosci. 2008; 28:11526–11536. [PubMed: 18987189]

Roth J, Olasunkanmi A, Ma TS, Carlson C, Devinsky O, Harter DH, Weiner HL. Epilepsy control following intracranial monitoring without resection in young children. Epilepsia. 2012; 53:334–341. [PubMed: 22242686]

Sahin NT, Pinker S, Cash SS, Schomer D, Halgren E. Sequential processing of lexical, grammatical, and phonological information within Broca's area. Science. 2009; 326:445–449. [PubMed: 19833971]

Sala-Llonch R, Bartres-Faz D, Junque C. Reorganization of brain networks in aging: a review of functional connectivity studies. Front Psychol. 2015; 6:663. [PubMed: 26052298]

Serafini S, Komisarow JM, Gallentine W, Mikati MA, Bonner MJ, Kranz PG, Haglund MM, Grant G. Reorganization and stability for motor and language areas using cortical stimulation: case example and review of the literature. Brain Sci. 2013; 3:1597–1614. [PubMed: 24961623]

Shah AK, Mittal S. Invasive electroencephalography monitoring: Indications and presurgical planning. Ann Indian Acad Neurol. 2014; 17:S89–94. [PubMed: 24791095]

Sillay KA, Rutecki P, Cicora K, Worrell G, Drazkowski J, Shih JJ, Sharan AD, Morrell MJ, Williams J, Wingeier B. Long-term measurement of impedance in chronically implanted depth and subdural electrodes during responsive neurostimulation in humans. Brain Stimul. 2013; 6:718–726. [PubMed: 23538208]

Skoe E, Krizman J, Anderson S, Kraus N. Stability and plasticity of auditory brainstem function across the lifespan. Cereb Cortex. 2015; 25:1415–1426. [PubMed: 24366906]

Smart O, Rolston JD, Epstein CM, Gross RE. Hippocampal seizure-onset laterality can change over long timescales: A same-patient observation over 500 days. Epilepsy Behav Case Rep. 2013; 1:56–61. [PubMed: 25667828]

Spencer DC, Sun FT, Brown SN, Jobst BC, Fountain NB, Wong VS, Mirro EA, Quigg M. Circadian and ultradian patterns of epileptiform discharges differ by seizure-onset location during long-term ambulatory intracranial monitoring. Epilepsia. 2016

Steinschneider M, Nourski KV, Kawasaki H, Oya H, Brugge JF, Howard MA 3rd. Intracranial study of speech-elicited activity on the human posterolateral superior temporal gyrus. Cereb Cortex. 2011; 21:2332–2347. [PubMed: 21368087]

Tcheng T, Hasulak N, Arcot Desai S, Crowder Skarpaas T, Archer S, Cao J. Clinical research use of the NeuroPace RNS System. American Epilepsy Society Annual Meeting Abst. 2015; 3:085.

Udden J, Bahlmann J. A rostro-caudal gradient of structured sequence processing in the left inferior frontal gyrus. Philos Trans R Soc Lond B Biol Sci. 2012; 367:2023–2032. [PubMed: 22688637]

Wu C, Evans JJ, Skidmore C, Sperling MR, Sharan AD. Impedance variations over time for a closed-loop neurostimulation device: early experience with chronically implanted electrodes. Neuromodulation. 2013; 16:46–50. discussion 50. [PubMed: 23136991]

Zatorre RJ, Fields RD, Johansen-Berg H. Plasticity in gray and white: neuroimaging changes in brain structure during learning. Nat Neurosci. 2012; 15:528–536. [PubMed: 22426254]

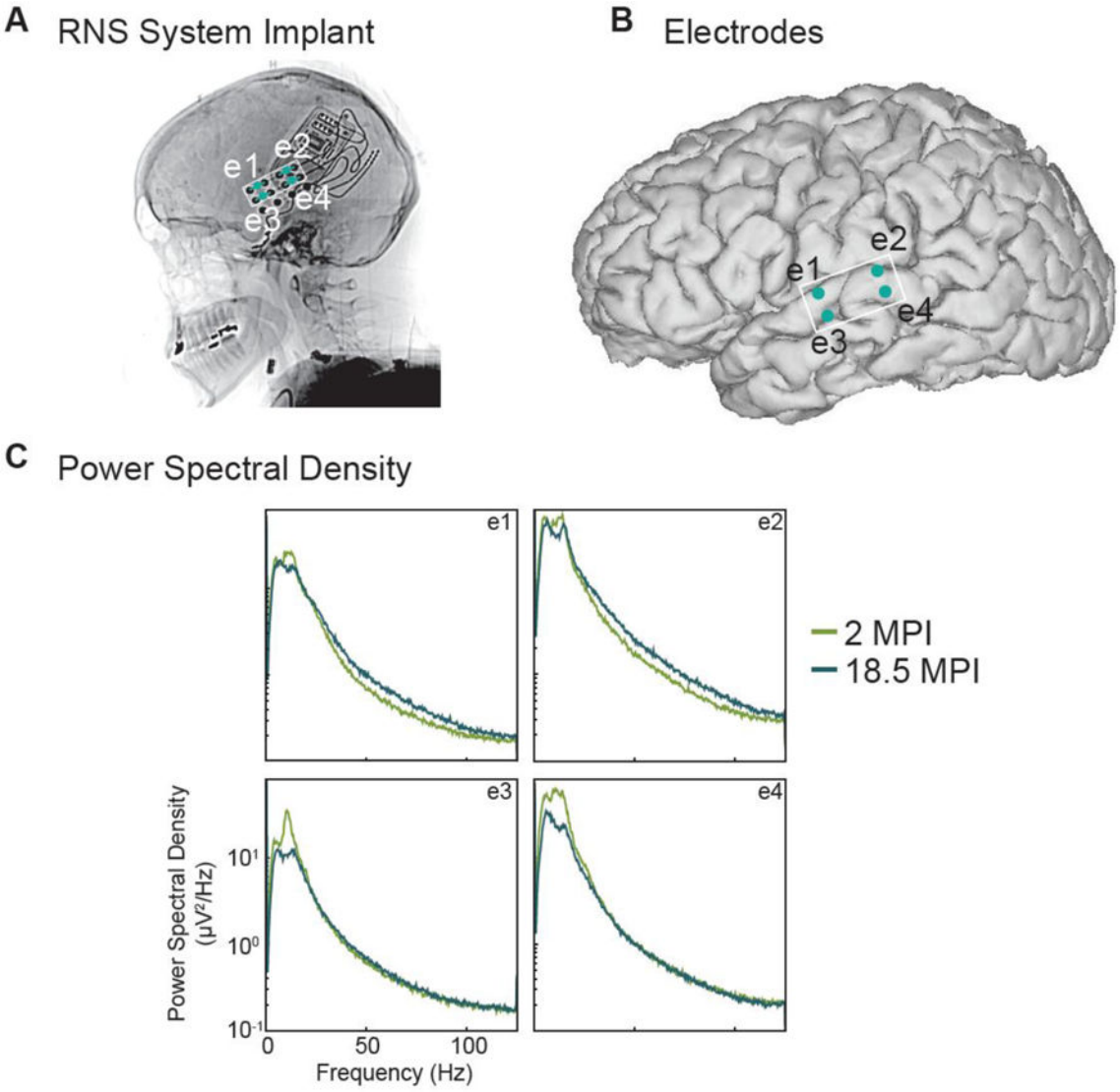

Figure 1.

Electrode characteristics of RNS System recordings from Wernicke's area. (A) Computed tomography (CT) scout image showing implanted RNS System. Blue electrodes (e1–4) show inferred locations of bipolar referenced signals. (B) Locations of RNS System electrodes on reconstructed cortical surface. (C) Power spectral density shows expected power law for both recordings and consistency across the two timepoints (2 and 18.5 months post-implant [MPI]).

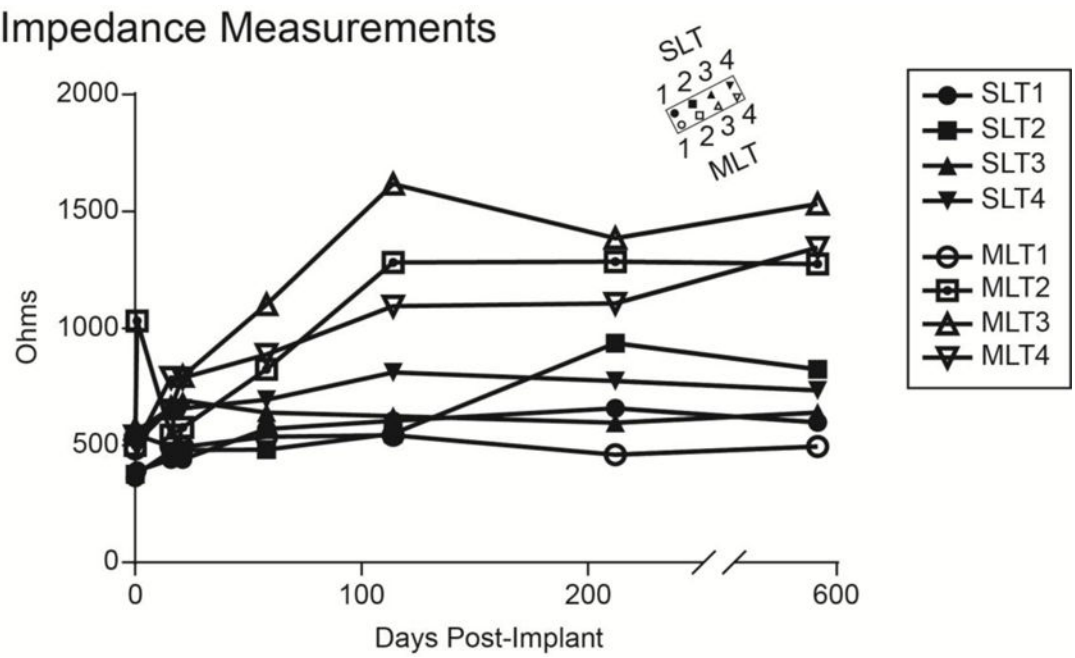

Figure 2.

Subject 1 RNS System lead impedances over time. Impedance measurements (Ohms) for the four electrode contacts of each cortical strip lead (lead labels: superior lateral temporal, ‘SLT’; middle lateral temporal, ‘MLT’; inset shows orientation in left lateral view as in Fig. 1A) are plotted as a function of days post-implant. Following an increase during the first 16 weeks after implantation, impedances stabilize in long-term follow-up. Normal lead impedances for the RNS System are 300–3000 Ohms.

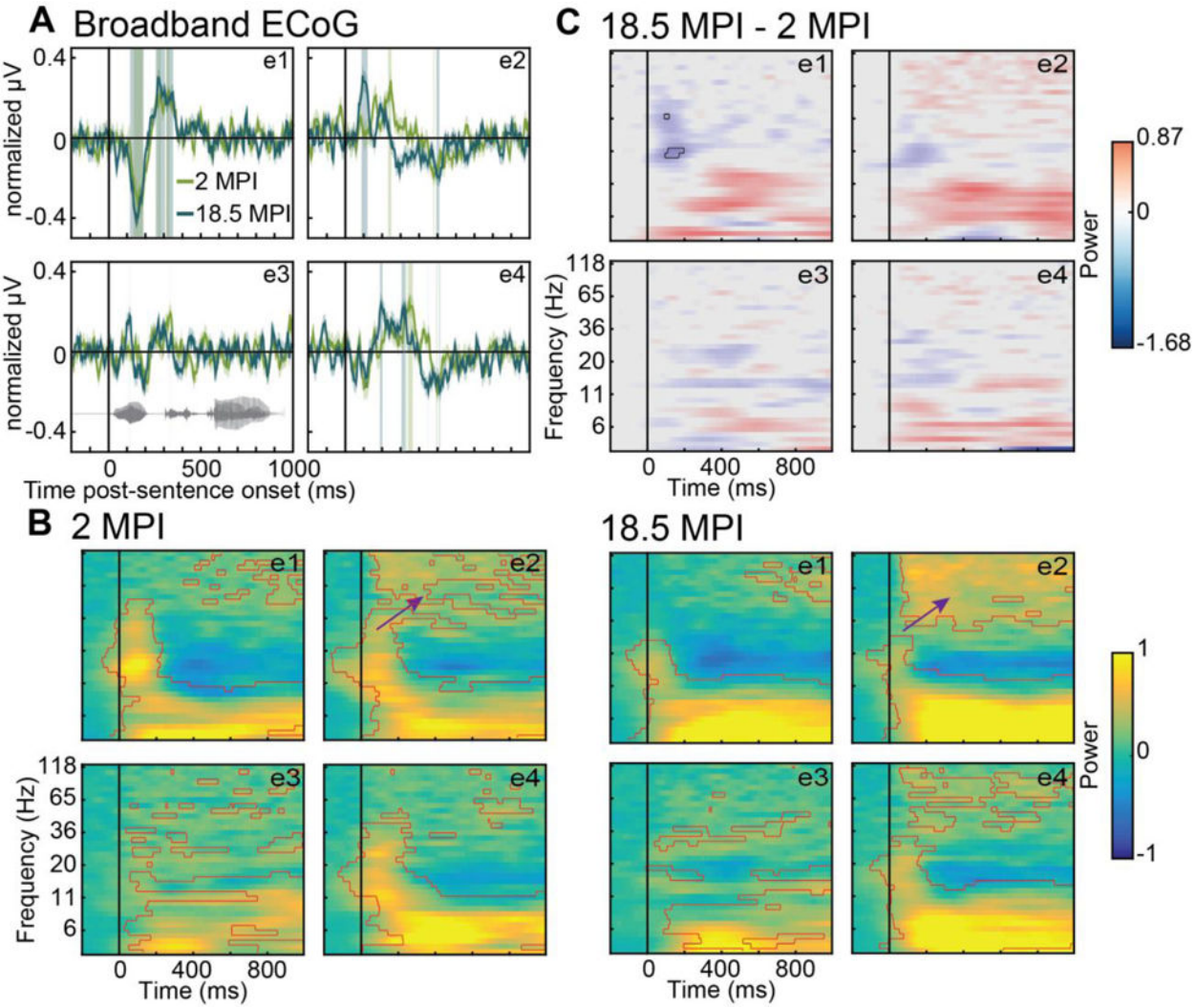

Figure 3.

Event-related potentials (ERPs) to average sentence onsets. (A) ERPs in the raw broadband signal. Electrode 1 (e1) shows a consistent negative peak ~150ms after sentence onset in both recordings. Shaded regions indicate significant deviations from baseline ($p<0.05$, corrected for timepoints). The gray waveform in the bottom-left panel is the sound wave for an example sentence. (B) Neural spectrogram of average auditory-evoked activity at 2 MPI (left) and 18.5 MPI (right). Red outlines indicate significant increases over baseline ($p<0.05$). Purple arrows illustrate increase in high-gamma activity locked to sentence onset. (C) Difference between 18.5 MPI and 2 MPI spectrograms from (B). Outlined region on e1 indicates the only region that showed significant differences across timepoints ($p<0.05$, corrected for timepoints and frequency bins). Color bar indicates normalized power.

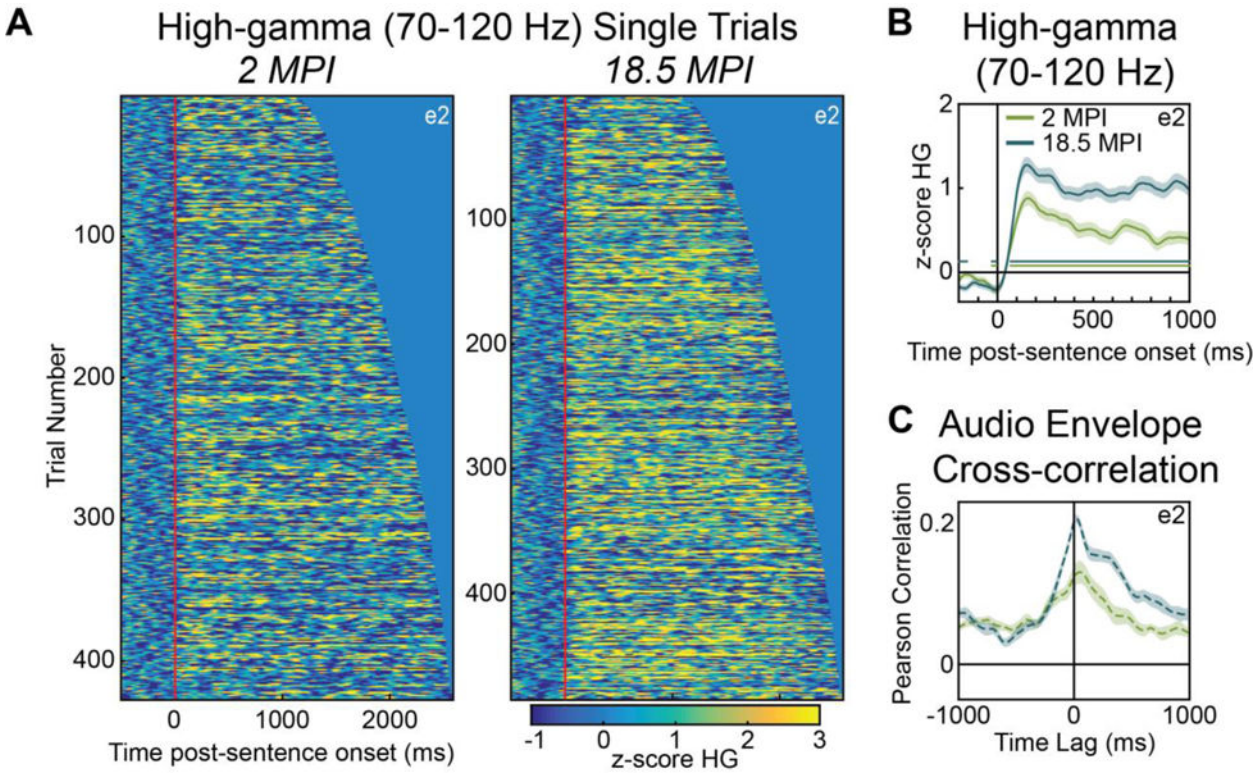

Figure 4.

High-gamma responses to sentence onsets. (A) Single-trial raster plots showing high-gamma (HG; 70–120 Hz) auditory evoked activity on electrode 2 (e2) at both 2 and 18.5 MPI. Trials sorted by sentence length. (B) Average ERPs show a consistent increase in HG power peaking ~150ms after sentence onset. Shaded regions indicate standard error of the mean. Blue and green bars indicate timepoints where responses are significantly different from zero ($p < 0.05$, corrected for timepoints). (C) Cross-correlation between HG signal and audio envelope reveals a peak correlation on e2 at short lags (~50ms) in both recordings.

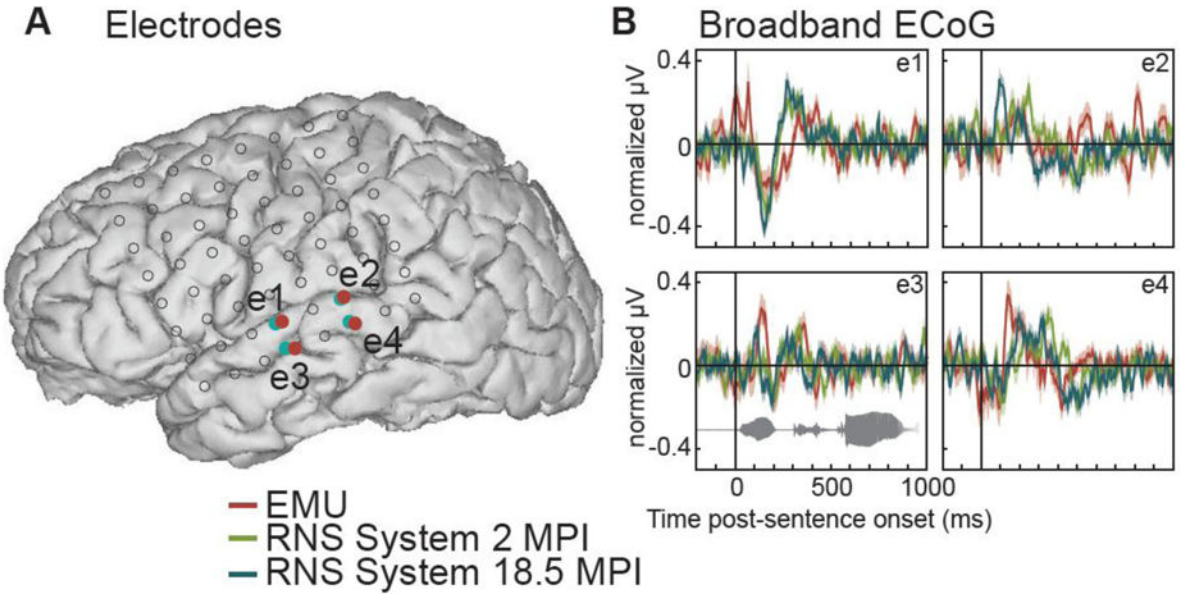

Figure 5.

Comparison between inpatient ECoG in the epilepsy monitoring unit (EMU) and RNS System recordings. (A) CT-registered locations of EMU (red) and RNS System (blue) electrodes. (B) ERPs in the raw broadband signal. Responses are qualitatively similar across all recordings, with minor differences in EMU recordings likely due to differences in electrode placement.

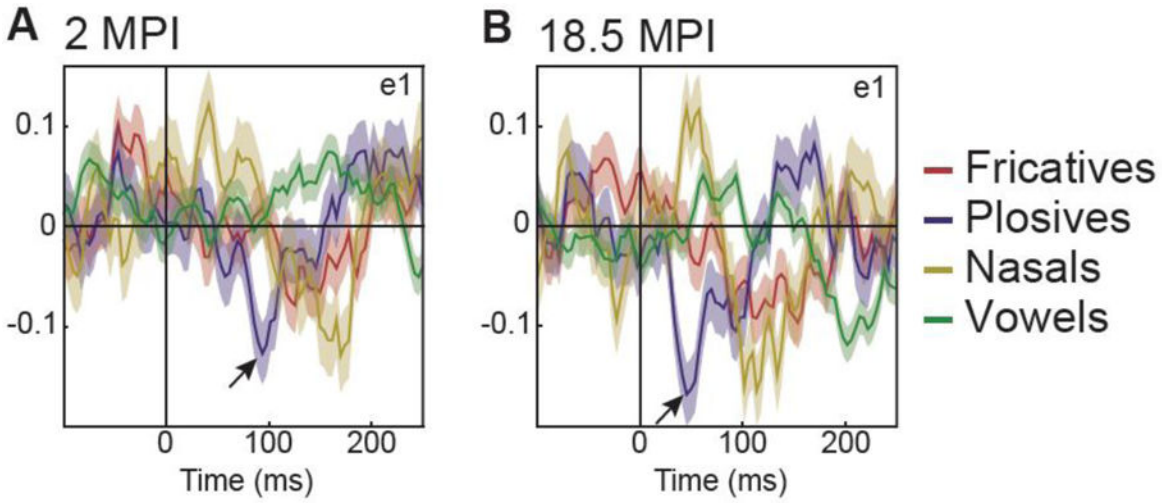

Figure 6.

Broadband ERPs to phonetic features are consistent across time. (A) ERPs to four phonetic feature classes show selectivity to plosives during an early negative peak at 2 MPI. (B) The same electrode shows a similar pattern of phonetic feature selectivity at 18.5 MPI. Shaded regions indicate standard error of the mean. The arrow illustrates the similar response for plosives relative to the other phonetic categories. Fricatives: e.g., /s/, /sh/, /z/; Plosives: e.g., /p/, /t/, /g/; Nasals: e.g., /m/, /n/, /ng/; Vowels: e.g., /aa/, /iy/, /uw/.

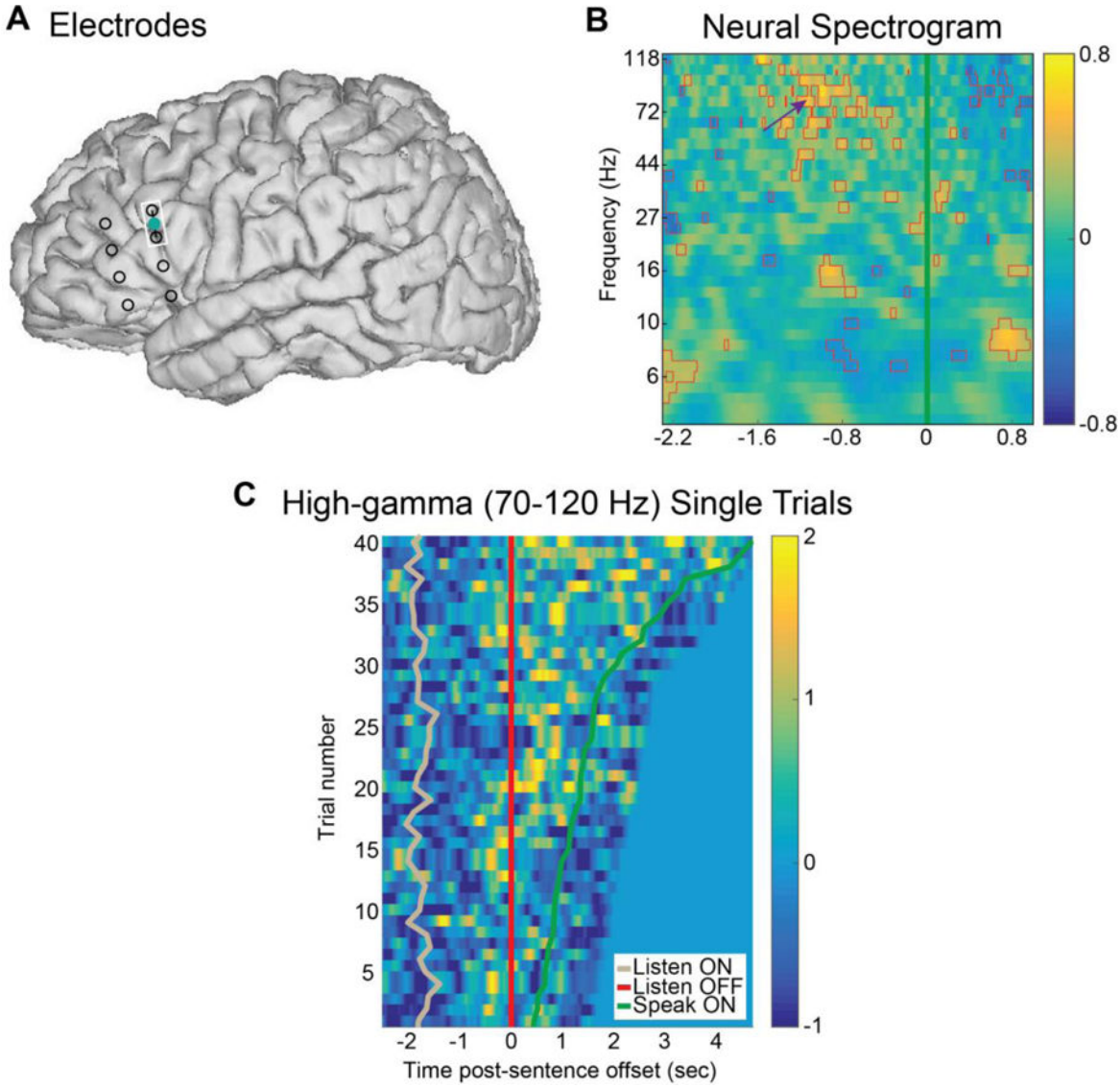

Figure 7.

RNS System recordings from Broca's area. (A) RNS System electrode locations (four bipolar channels) shown as open circles on a reconstructed cortical surface. The inferred location of relevant activity in subsequent panels is shown in blue. (B) Neural activity spectrogram aligned to speech-onset for the bipolar channel highlighted in A, averaged across trials with reaction time less than 5 seconds (N=40). Frequency bands were normalized (z-scores, indicated by the color axis) across trials. There is a large increase in HG power in the seconds leading up to speech onset (purple arrow). Red outlines indicate significant increases over baseline (one-way z-test $p<0.05$). (C) Single-trial raster plot showing HG activity (z-score indicated by the color axis) from the same channel, with trials sorted by reaction time. HG consistently increases toward the end of the sentence and remains elevated after the prompt, until suddenly decreasing at speech onset.

Table 1

Pearson correlations across recording sessions for mean timecourse from [−500 1000]ms for each RNS System broadband ECoG channel. Timecourses were averaged across ~500 trials and bootstrapped 1000 times to determine 95% Confidence Intervals (CI).

Channel	r-value	p-value	95% CI
1	0.82	3.60e-93	[0.77 0.86]
2	0.26	4.89e-07	[0.18 0.34]
3	0.30	3.02e-09	[0.21 0.39]
4	0.51	6.39e-26	[0.41 0.58]
All	0.53	9.18e-109	[0.47 0.58]

Table 2

Pearson correlations across recording sessions for mean spectrogram from [−1000 2000]ms for each RNS System channel. Timecourses were averaged across ~500 trials and bootstrapped 1000 times to determine 95% CI.

Channel	r-value	p-value	95% CI
1	0.82	0	[0.81 0.82]
2	0.84	0	[0.84 0.85]
3	0.57	0	[0.56 0.58]
4	0.80	0	[0.79 0.81]
All	0.79	0	[0.77 0.79]